

# Pluvio: Assembly Clone Search for Out-of-domain Architectures and Libraries through Transfer Learning and Conditional Variational Information Bottleneck

Zhiwei Fu  
zhiwei.fu@queensu.ca  
Queen's University  
Kingston, Ontario, Canada

Steven H. H. Ding  
steven.ding@queensu.ca  
Queen's University  
Kingston, Ontario, Canada

Furkan Alaca  
furkan.alaca@queensu.ca  
Queen's University  
Kingston, Ontario, Canada

Benjamin C. M. Fung  
ben.fung@mcgill.ca  
School of Information Studies, McGill  
University  
Montreal, Quebec, Canada

Philippe Charland  
philippe.charland@ecn.forces.gc.ca  
Defence Research and Development  
Canada (DRDC)  
Ottawa, Ontario, Canada

## ABSTRACT

The practice of code reuse is crucial in software development for a faster and more efficient development lifecycle. In reality, however, code reuse practices lack proper control, resulting in issues such as vulnerability propagation and intellectual property infringements. Assembly clone search, a critical shift-right defence mechanism, has been effective in identifying vulnerable code resulting from reuse in released executables. Recent studies on assembly clone search demonstrate a trend towards using machine learning-based methods to match assembly code variants produced by different toolchains. However, these methods are limited to what they learn from a small number of toolchain variants used in training, rendering them inapplicable to unseen architectures and their corresponding compilation toolchain variants.

This paper presents the first study on the problem of assembly clone search with unseen architectures and libraries. We propose incorporating human common knowledge through large-scale pre-trained natural language models, in the form of transfer learning, into current learning-based approaches for assembly clone search. Transfer learning can aid in addressing the limitations of the existing approaches, as it can bring in broader knowledge from human experts in assembly code. We further address the sequence limit issue by proposing a reinforcement learning agent to remove unnecessary and redundant tokens. Coupled with a new Variational Information Bottleneck learning strategy, the proposed system minimizes the reliance on potential indicators of architectures and optimization settings, for a better generalization of unseen architectures. We simulate the unseen architecture clone search scenarios and the experimental results show the effectiveness of the proposed approach against the state-of-the-art solutions.

## CCS CONCEPTS

• **Computer systems organization** → **Embedded systems**; *Redundancy*; Robotics; • **Networks** → Network reliability.

## KEYWORDS

Firmware, IoT Vulnerabilities, Code Similarity, Sentence Transformer

## 1 INTRODUCTION

The concept of copying code is crucial in software development and is commonly referred to as “code reuse”, as noted in [30, 43]. This involves using parts of software that encapsulate functionality or lines of code from pre-existing systems [30]. Implementing a high-quality code reuse policy can lead to faster and more efficient development, as well as more maintainable software [43]. In reality, however, many code reuse practices lack proper quality management, resulting in issues such as vulnerability propagation and intellectual property infringements. The complexity of the software supply chain, coupled with the widespread use of open-source third-party libraries, exacerbate this issue. It is not uncommon to discover multiple instances of the same vulnerable code across firmware releases<sup>1</sup>.

Assembly clone search is a critical shift-right defence mechanism that aims to identify vulnerable code resulting from reuse in released executables. It is designed to locate known vulnerable code in released software through searching. It has proven effective in various security-related challenges, including identifying software plagiarism [34], detecting injected malware [10], searching for existing vulnerabilities in software or firmware images of IoT devices [9, 16], and identifying performance issues, such as increased resource consumption, and in patches [24]. For a practical clone search system, a scalable and robust matching approach is necessary to compare diverse assembly code variants of the same source code, generated by different compilers and optimization techniques specific to different processor architectures [16, 23, 38].

Recent studies on assembly clone search demonstrate a trend toward using machine learning-based methods to match assembly code variants produced by different toolchains. This is due to the inefficiency and limited coverage that result from relying solely on human knowledge [23]. Deep learning models, such as GEMINI [49], ASM2VEC [17], and the ORDER MATTERS model [51], are utilized to create assembly embeddings by leveraging assembly functions and Control-Flow Graphs (CFGs). In addition, Natural Language Processing (NLP) strategies are employed in SAFE [35] and PALMTREE [33] to improve efficiency and generalizability in cross-platform detection.

<sup>1</sup>See: The Firmware Supply-Chain Security is broken: Can we fix it?

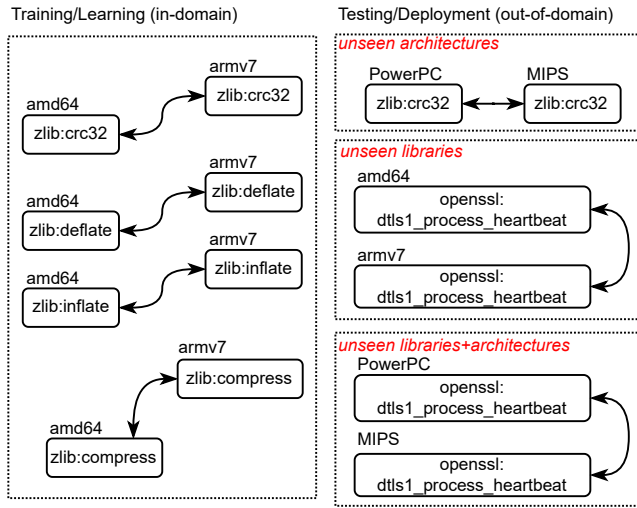


**Figure 1: When deploying assembly clone search engines, out-of-domain issues arise. This occurs when certain architectures and libraries are not accessible during the training process, which is limited by access to compilers and the difficulty of encompassing all potential architectures. The objective is to acquire knowledge from a specific set of architectures and libraries, and then apply it to previously unseen ones.**

These methods allow models to learn directly from data. However, they are generally limited to what they can learn from, i.e., a small number of toolchain variants used in training. For instance, the ORDER MATTERS model [51] can accurately match x86 and ARM assembly code after training on known pairs of assembly code variants. Nevertheless, a range of toolchain variants exists in the wild, including ARMv4, MIPS series, and Motorola MC68 series. Many of these low-resource or proprietary processor toolchains limit the capacity to generate training data, rendering the system inapplicable to unseen architectures and their corresponding compilation toolchains. Moreover, systems such as PALMTREE and ASM2VEC are trained and tested on different function pairs from the same set of libraries, leading to performance degradation when making inferences on unseen libraries. We term this practical challenge in assembly clone search **out-of-domain architecture and libraries**, as illustrated in Figure 1. Assembly clone search faces significant challenges as a shift-right solution, due to this issue. Certain hardware vendors, for instance, develop firmware for various devices such as webcams, VoIP phones, and wireless routers using the same code base, but each device has a different CPU architecture [39].

At its core, the previously mentioned problem with current learning-based approaches stems from their sole reliance on task-specific data, without incorporating the broader knowledge of human experts in assembly code. Consider a reverse engineer who can begin comprehending an assembly code fragment of a new processor architecture, without consulting the manual. This individual has a general understanding of how assembly code operates and can identify similarities in instructions compared to those they already know. Incorporating such expert knowledge can aid in addressing

the limitations of the existing learning-based approaches. A reverse engineer does not simply learn from “assembly code,” but rather through years of education and practical experience. In machine learning, this falls within the transfer learning paradigm for domain adaptation. Natural Language Processing (NLP) techniques, including ChatGPT models, have exhibited tremendous accomplishments in transfer learning. These models excel at comprehending natural language text data in general and solving domain-specific tasks, such as programming, through downstream training.

This study simulates real-world scenarios of out-of-domain assembly clone search and explores the potential of utilizing large-scale language models pre-trained on general text data. Unlike previous models that solely rely on assembly code, such as the ORDER MATTERS model, our study employs pre-trained models on natural language text data and treats assembly code as text data. By being trained on a small number of assembly code pairs based on x86 and ARM, some pre-trained models demonstrate high accuracy (>85%) in matching unknown architectures, such as MIPS and PowerPC. We further improve the model’s performance by considering the limitations of the pre-trained model: **L1 - sequence length limit** and **L2 - information compression**.

To tackle L1, we propose the *Removal* module, a reinforcement learning agent that aims to eliminate noise tokens from assembly code. While a typical pre-trained natural language model is limited by a sequence length cap of 800 words, an assembly function can be considerably longer than regular text paragraphs. Function inlining, compiler-specific injected code, and code duplication induced by the compiler optimization process expose substantial opportunities to effectively increase the sequence length, while retaining the crucial elements of the code sequence as the input to the pre-trained natural language model. For L2, we propose modifying the Variational Information Bottle (VIB) [4, 46] learning method to compress the information learned about the code architecture and optimization settings. Since the model should be capable of matching code of unseen architectures, we treat the assembly code’s architectures and optimizations as nuisance information. The goal of the learning is to “forget” this information and minimize the input information regarding those factors. In this paper, we make the following contributions:

- We propose to integrate common human knowledge into the learning process for assembly code similarity. We adopt pre-trained natural language models on text data using the transfer learning paradigm, where assembly code is treated as plain text data.
- In order to overcome the sequence length limitation of the pre-trained natural language model (L1), we propose using a reinforcement learning agent that is capable of eliminating noisy and redundant tokens via a policy gradient algorithm.
- In order to enhance the model’s resilience to out-of-domain architectures and libraries (L2), we introduce a novel approach: Conditional Variational Information Bottleneck (CVIB) learning, where conditions are used only during the training step. This method ensures that the model minimally relies on input information that could serve as indicators of architectures and optimization settings.

- We simulate the real-life out-of-domain scenarios and benchmark state-of-the-art methods for clone search. Our result demonstrates the effectiveness of transfer learning, the proposed *Removal* module, and the new CVIB (conditions in training only) approach<sup>2</sup>.

The rest of this paper is structured as follows. Section 2 provides a more thorough review of the relevant state-of-the-art methods for assembly code similarity detection. Section 3 elaborates the general design of *Pluvio*. Section 4 presents our experimental setup and results. Finally Section 5 concludes this paper.

## 2 RELATED WORK

Assembly code similarity detection has important cybersecurity applications. Traditionally, structural or syntactic features/representations such as CFGs from assembly code, and use them to match two assembly code fragments by calculating their similarity degrees. The shortcomings of these methods are their high computational cost and inefficiency. Recent techniques use an alternative way to extract representations from assembly functions. They automatically produce *embeddings*, which are real-valued feature vectors [23], from input assembly code. Xu *et al.* [49] propose a GNN-based model, called GEMINI, which uses extracted graph embeddings for annotated CFG blocks (a CFG that has nodes annotated with particular fundamental block attributes [23]) of assembly functions for detection. However, the input features for this method are still manually selected, which is ineffective and time-consuming, especially for assembly code for different architectures and from different vendors. Research attention is now shifting to semantic similarity, which captures if the functionalities of two compared assembly code fragments are identical [23]. Other techniques rely on instruction or raw byte co-occurrence rather than manually selected features [23].

Hence, people apply Natural Language Processing (NLP) to generate assembly code embeddings. In brief, word co-occurrence can be captured in word embeddings, so the embedding of a whole sentence can be built based on it. Zuo *et al.* [52] adopt an analogous strategy, considering a token as a word and a block as a sentence, and encode the semantic vector of a phrase using LSTM. Unlike the aforementioned approaches, Ding *et al.* [17] build ASM2VEC. It uses the PV-DM model [32] to concurrently produce instruction embeddings and an embedding for the function comprising these instructions to identify comparable functions in assembly code. ASM2VEC [17] overcomes the problem in recent works that fail to consider the relationships between features and identify those unique patterns that can statistically distinguish assembly functions. However, hardware platforms and systems have various specifications and requirements. Thus, when assembly programs comply with different hardware platforms, they have different architectures and they are not compatible with each other. In this case, even though ASM2VEC leads a promising way to handle assembly code, it loses generalizability, since it fails to pass the cross-architecture test. Massarelli *et al.* [35] utilize strategies in the NLP domain as well and propose the SAFE model, as an extended variation of GEMINI. It uses the word2vec model to create the embedding of assembly functions and a self-attentive neural network to generate block embeddings. It was trained by millions of lines of assembly code.

<sup>2</sup>source code and data will be publicly available if the paper moves to the next stage

Although this method achieves higher efficiency and generalizability than prior work, as it detects stripped and cross-architecture assembly code, it leaves much room to improve.

Li *et al.* [33] propose a BERT-based model called PALMTREE, an assembly language model pre-trained by three self-supervised tasks on large-scale datasets to generate embeddings of instructions for similarity detection. Unlike previous methods, it divides instructions into precise fundamental components. PALMTREE outperforms previous methods in outlier detection and basic block similarity search, but it still fails to consider the real-world testing cases of assembly codes that are compiled for different architectures, vendors, and optimizations. Realizing this problem, Yu *et al.* [51] propose a semantic-aware neural network, the ORDER MATTERS method. It is pre-trained by three different levels of tasks. A BERT model extracts semantic-aware embeddings from blocks and is then followed by a GNN model that collects structural-aware embeddings. Moreover, they use a CNN model on adjacent matrices of CFGs to capture the order information as an order-aware embedding. At last, an MLP layer is used to concatenate all embeddings to compute the final graph embedding. The ORDER MATTERS method [51] outperforms many previous approaches and is somewhat robust for cross-architecture. Nevertheless, it only supports two different platforms (x86 and ARM) and it does not fulfil our standards, since it still performs poorly in out-of-domain testing.

## 3 RESEARCH METHODOLOGY

We implement a novel and robust model for assembly code clone search at the semantic/functional level with high accuracy against out-of-domain architectures and libraries, as well as inlining functions with compiler-injected code. Our proposed model, named *Pluvio*, has the following components: a pretrained natural language model based on MPNet [44], a tokenizer, denoted by *MPNetTokenizer*, and an encoder denoted by *MPNetEmbedder*. Furthermore, it has a reinforcement learning agent model, denoted by *Removal*, to remove noise tokens from inlining functions and injected code, and an encoder and decoder based on the novel technique, Conditional Variational Information Bottleneck (CVIB), for conditions in training only, denoted by *CVIBEncoder* and *CVIBDecoder*, to capture the key representations of instructions regardless of their architectures, libraries, and optimizations. Moreover, we train *Pluvio* on a set of assembly function pairs and utilize three different loss functions, cosine similarity loss [41], denoted as  $L_{cos\_sim}$ , reinforce learning loss, denoted as  $L_{RL}$ , and information loss, denoted as  $L_{CVIB}$ . Finally, we apply  $\beta_1$  and  $\beta_2$ , known as Lagrange parameters, to control the learning rate of  $L_{RL}$  and  $L_{CVIB}$ , so the overall loss function,  $L_{pluvio}$ , is defined as

$$L_{pluvio} = L_{cos\_sim} + \beta_1 \cdot L_{RL} + \beta_2 \cdot L_{CVIB} \quad (1)$$

The following sections thoroughly explain each of these components and Figure 2 depicts an overview of the *Pluvio* architecture.

The input for training *Pluvio* is a pair of assembly instruction sequences denoted by  $I_a$  and  $I_b$ , with the ground truth  $y_{actual}$  that is either 1 (similar) or 0 (dissimilar). The output  $sscore$  is the similarity score of the pair  $I_a$  and  $I_b$ . The goal is to learn a function  $f$  that is able to encode  $I_a$  and  $I_b$  into a pair of fixed-length encodings  $Z_a$  and  $Z_b$ . Then, the function  $f$  can map two assembly instructions to their similarity score  $sscore$ :  $f : (I_a, I_b) \in \mathbb{D} \rightarrow (Z_a, Z_b) \rightarrow sscore \in \mathbb{R}$

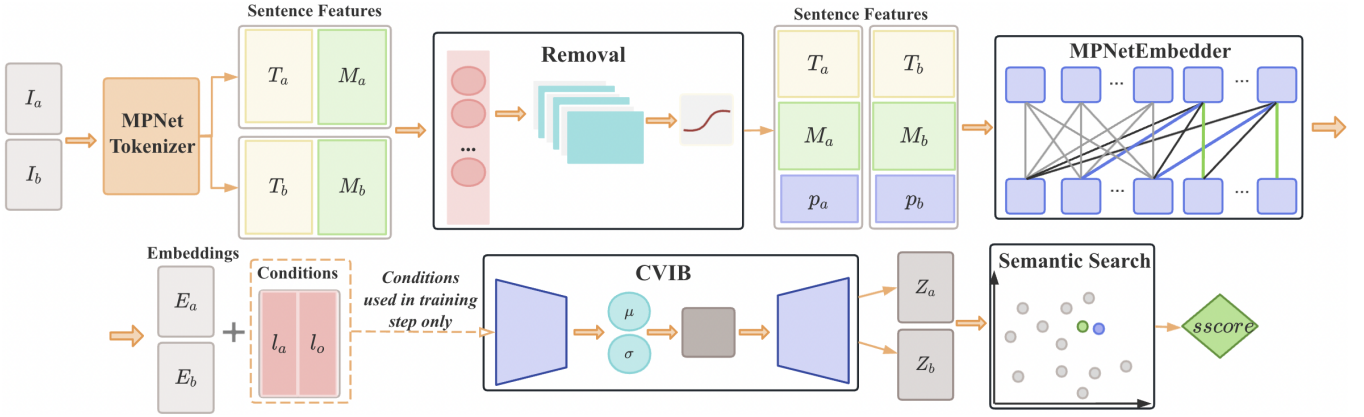


**Figure 2: The Structural Overview of *Pluvio*.** A pair of assembly instruction sequences  $I_a$  and  $I_b$  are fed into the MPNet tokenizer that outputs the tokens ids ( $T_a$  and  $T_b$ ) and attention masks ( $M_a$  and  $M_b$ ) for both instructions. Then, the *Removal* agent model will select the optimal tokens by removing the noise tokens from functions inlining and compiler-injected code. Afterwards, based on embeddings  $E_a$  and  $E_b$  created by the MPNet Encoder, a CVIB Encoder with conditions  $l_o$  and  $l_a$  will generate instruction encodings  $Z_a$  and  $Z_b$  by removing the nuisance information from the optimizations and architectures. At last, the semantic search method is adopted to calculate the similarity score *sscore* of two encodings.

where  $sscore \in [0, 1]$ . The set  $\mathbb{D}$  represents the pair-wise out-of-domain testing data from different architectures, libraries, or both (as illustrated in the right half of Figure 1).

### 3.1 Pre-trained Natural Language Model

In the NLP domain, the semantic similarity of a pair of texts in natural languages can be determined by calculating the similarity degree of their embeddings [2]. We capture tokens from assembly instructions, rather than from their CFGs and their adjacency matrices, to reduce the effect of noisy information from various architectures, libraries, and compiler optimizations [33]. Similar to natural languages, instructions can be treated as a sentence and tokens as words. Thus, we feed our pre-trained natural language model a long string (an instruction sequence of one assembly function) as input and then either tokenize or encode it for the *sscore* calculation.

As a breakthrough in language modelling introduced in 2017, a Transformer [48] consists of a point-wise and fully connected encoder and decoder. It uses a multi-head attention algorithm to connect the encoder and decoder, and constructs representations of its input and output purely utilizing self-attention, without convolution or a sequence-aligned recurrent neural network [48]. Taking advantage of Transformer, BERT [15], mainly pertained by masked language modelling (MLM), shows its great potential in dealing with NLP problems [41]. However, MLM effectively uses the bidirectional context of masked tokens, but it overlooks the dependence between the masked tokens [50]. Introduced by XLNet [50], the permuted language modelling (PLM) is another powerful pre-training tool that captures the dependencies among tokens, but loses positional information of the full sentence [44]. To leverage the strengths of MLM and PLM and alleviate their shortcomings, masked and permuted language modelling (MPNet) [44] is proposed in 2020. In addition to considering the interdependence of the predicted tokens using PLM, MPNET also uses the positions of all tokens as input to enable the model to know the positional information for all

tokens, which addresses the issues in BERT [15] and XLNet [44, 50]. In addition, MPNet is pre-trained on a huge text corpus, around 160GB of data.

To understand the mechanism of MPNet [44], we first need to know how MLM and PLM work. While training, MLM masks predictable tokens and moves them to the rightmost position of the whole input sentence. For PLM, it will first permute tokens of the sentence and select the rightmost tokens as predicted tokens. Based on this, both MLM and PLM have a unified view that the predicted tokens are all put at the end of input sentences [44]. Employing the techniques in MLM and PLM, MPNet [44] has the structure shown in Figure 3. MPNet tries to maximize the following objective while pre-training model  $\theta$  [44].

$$E_{z \in Z_n} \sum_{t=c+1}^n \log P(x_{z_t} | x_{z < t}, M_{z > c}; \theta) \quad (2)$$

As can be seen in Figure 3,  $X_n$  is the input token and  $P_m$  is the corresponding position information. The permuted input sequence is  $X_a \dots X_d$  and  $c$  in Equation 2 denotes the number of non-predicted tokens. Thus, the predicted part is  $X_c \dots X_d$  and the rest of the tokens ( $x_{z < t} = X_a \dots X_b$ ) are the non-predicted. MPNet utilizes mask tokens  $[m]$  of the predicted part as input as well, corresponding to the  $m_{z > c}$  part in the objective equation. Then, MPNet extracts representations from the input tokens ( $X_a \dots X_b [m] \dots [m]$ ), by bidirectional modelling [15, 44], shown by the grey lines in the Transformer in Figure 3. The blue and green lines in Figure 3 represents the two-stream (content and query) self-attention [50] technologies that MPNet uses to predict tokens ( $X_c \dots X_d$ ) [44]. Leveraging the advantages of MLM and PLM, MPNet uses all the position information to obtain an overall view of the input [44], which makes it an ideal language model to extract semantic/functional representations from instructions.

We extract the first MPNet model from a pre-trained sentence transformer published by Hugging Face [25], called *all-mpnet-base-v2* model. *all-mpnet-base-v2* is built based on the *MPNet-base* [44]

and fine-tuned on a one billion pairs dataset using a contrastive learning objective (train the model to identify which of a group of randomly picked other sentences was genuinely matched with a specific phrase in the dataset given a sentence from the pair) [19]. It contains both *MPNetTokenizer* and *MPNetEmbedder*.

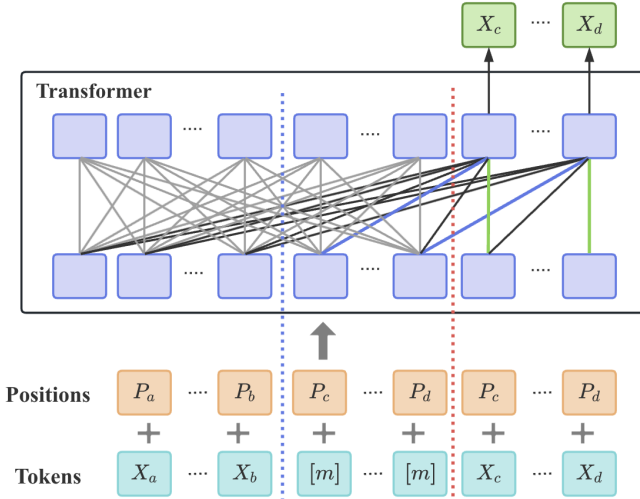


**Figure 3: The structural illustration of the MPNet Model. The leftmost inputs are non-predicted tokens and the rightmost tokens are selected as predicted tokens. The middle masks are the mask tokens of the predicted tokens. All the tokens along with their corresponding positions are fed into the model. Utilizing the MLM and PLM methods and the two-stream self-attention technologies, the MPNet model extracts representations via a bidirectional model.**

### 3.2 Subsequence Removal

*Removal* aims to remove the noise tokens from assembly code, caused by function inlining and compiler-injected codes. Function inlining [3], also known as function inline expansion or function inlining optimization, is a compiler optimization method that substitutes the actual body of the function for a function call at the call site during compilation [11, 28]. This involves inserting the function’s code at the call site rather than creating a separate function call instruction and jumping to the function’s address in memory, therefore avoiding the cost of the function call and enhancing efficiency [21, 23, 28]. Also, this method can remove the time and memory overheads that are caused when calling functions, due to the stacking of arguments, the saving and restoring of registers, and the jumping to and from the function [26]. Moreover, some compilers only allow the inlining of functions that have already been defined in the file. Others first parse the full file so that functions defined after a call site may also be inlined. Yet other compilers permit the inlining of functions that have been declared in separate files [13]. Programmers have little or no control over which functions are inlined [11]. Besides, compiler-injected code is another problem. Similar to functions inlining, compilers may replace or inject additional code into the original function during compilation.

This is frequently done to incorporate specific language features or for optimization considerations. A compiler could inject extra code, for instance, to optimize memory utilization or boost speed. Additionally, the compiler could add code to carry out bounds checking, memory access validation, or other security checks to protect the program.

To remove the above noise tokens from the instruction sequence tokens, we place the *Removal* model following the MPNet tokenizer, which adopts Reinforcement Learning (RL). Reinforcement learning, as a branch of machine learning, is concerned with teaching an agent how to operate in a given environment in a way that would maximize a cumulative reward signal, known as a discounted reward, denoted by  $G_t$ . In reinforcement learning, an agent model performs an action in the environment and receives feedback in the form of rewards or punishments. The agent can learn an optimal policy by the time the projected cumulative reward reaches the maximum over time [27].

The agent is related to its environment in the traditional RL paradigm through observation/perception and action. Typically, the agent consists of a set of environment states, denoted as  $S$ , and a set of actions, denoted as  $A$ . Then, it receives an input,  $o$ , the observation of the environment’s current state,  $s$ , at each stage of interaction [27]. The type of observation we employed is referred to as complete observation, which gives the agent comprehensive knowledge of the condition of the environment. The agent then decides which action ( $a$ ) it produces as output and will get an immediate reward,  $R$ , once making an action.  $R_d(s, s')$  defines the reward after transition from  $s$  to  $s'$  with action  $a$ . Moreover, the environment will typically alter as a result of the agent’s action. The agent is informed of the immediate reward and the following  $s'$  after making a decision, but is not informed of the action that would have been in its greatest long-term interest [27]. While making decisions about actions, the agent first distributes probabilities on each possible action and chooses the one with the largest probability. In this case, the agent actively gains relevant experience regarding the potential environmental states, actions, and rewards. Therefore, finding the optimal policy  $\pi$  for choosing actions that maximize a long-term reward signal is the aim of a reinforcement learning agent. Given the condition of the environment at time  $t$ , the policy is often expressed as a probability distribution across possible actions [27, 45]. The formula of the policy below

$$\pi(a, s) = P(a_t = a \mid s_t = s) \quad (3)$$

shows the probability distribution  $P$  if agent takes action  $a$  given the states  $s$  at time  $t$ .

However, our agent plays only a *one-step* ( $t = 1$ ) game, which means there are no iterations of actions, discounted factors, etc. Figure 4 shows the architecture of *Removal*. Overall, the model consists of two layers and an activation function. The inputs, or observations/perceptions, of the agent model, are the environment states  $o = s = S$ . Observations are the token IDs in our case, denoted by  $T$ , of tokenized instructions (the number of  $T$  equals the max sequence length, denoted by  $LS_{max}$ , of *MPNetTokenizer*). In other words, our agent model has a set of  $LS_{max}$  independent decisions to choose from and each of the decisions (tokens) is a distributed probability

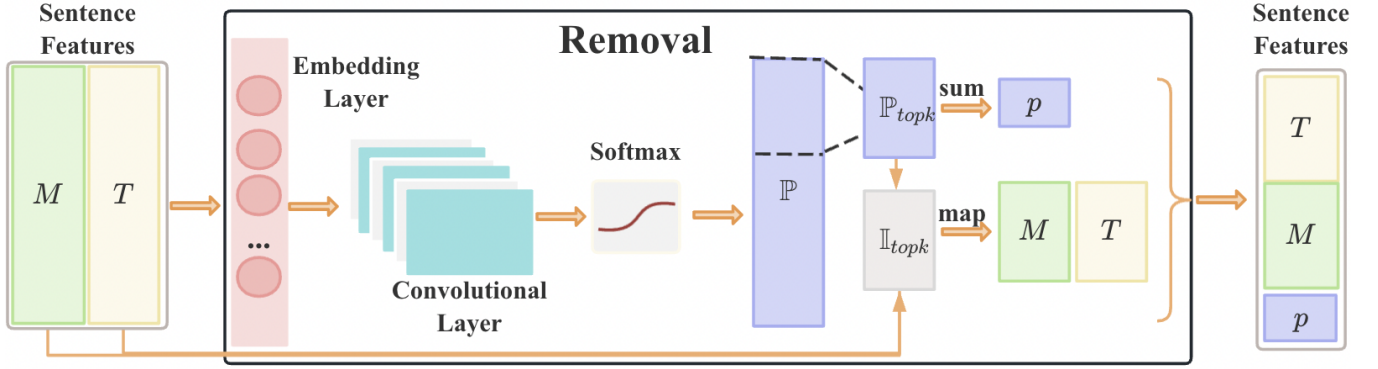


**Figure 4: The Structural Illustration of the *Removal* Agent Model.** The token ids and attention mask tokens are fed into the *Removal* agent model consisting of an embedding layer, a convolutional layer, and a softmax activation function. To remove the noise tokens of the inlining functions and injected code in instructions, the agent model selects top-k tokens and adds them to the sentence features as the output.

and the whole set of distributions is denoted by  $\mathbb{P}$ . From Figure 4, token IDs  $T$  are fed into the embedding layer of *MPNetEmbedder*, then into the 1D convolution layer ( $in\_channels=768$ ,  $out\_channels=1$ ,  $kernel\_size=3$ ,  $padding="same"$ ). After applying the Softmax function, we obtain the probability distribution  $\mathbb{P}$  in the same shape as  $T$ .

Afterwards, instead of taking one optimal decision from  $\mathbb{P}$ , our agent selected the top-k tokens ( $k$  equals the input sequence limit of the *MPNetEmbedder*) with the largest probabilities, denoted by  $\mathbb{P}_{topk}$ , as output policy,  $\pi$ , and also outputs indices of  $\mathbb{P}_{topk}$ , denoted by  $\mathbb{I}_{topk}$ . It then maps  $\mathbb{I}_{topk}$  on  $T$  and  $M$  to extract the corresponding token ids and attention masks. Additionally, every batch's values in  $\mathbb{P}_{topk}$  are summed up and we have the summed probability distribution, denoted by  $p$ . Last, *Removal* outputs features ( $T$ ,  $M$ , and  $p$ ). As one inserted model after the *MPNetTokenizer*, the *Removal* is trained with the MPNet model.

### 3.3 Cosine Similarity Loss

To train *Pluvio*, we adopt the cosine similarity loss [41] as one of our loss functions. In the NLP domain, it is frequently used to gauge textual similarity [22]. The measure of cosine similarity is the cosine of the angle between the vectors, or the dot product of the vectors divided by the product of their lengths and the similarity degree value is always in the range  $[-1, 1]$ . The mathematical expression of cosine similarity given a pair of instruction embeddings,  $E_a$  and  $E_b$  that have  $i$  components is [1]

$$\cos\_sim(E_a, E_b) = \frac{E_a \cdot E_b}{\|E_a\| \cdot \|E_b\|} = \frac{\sum_{i=1}^n E_{ai} E_{bi}}{\sqrt{\sum_{i=1}^n E_{ai}^2} \sqrt{\sum_{i=1}^n E_{bi}^2}} \quad (4)$$

The loss function then computes the Mean Squared Error (*MSE*) to measure the difference between the actual label,  $y_{actual}$ , and  $\cos\_sim(E_a, E_b)$  as the cosine similarity loss [41]. The mean squared error is an assessor for classifiers or predictors, which evaluates the average squared variation between the vector value of the actual label [7]. Our objective is to minimize the cosine similarity loss [41],

which we compute by

$$\begin{aligned} L_{\cos\_sim} &= MSE(y_{actual} - \cos\_sim(E_a, E_b)) \\ &= \|y_{actual} - \cos\_sim(E_a, E_b)\|^2 \\ &= \left\| y_{actual} - \frac{E_a \cdot E_b}{\|E_a\| \cdot \|E_b\|} \right\|^2 \end{aligned} \quad (5)$$

### 3.4 Reward Function and Policy Gradient

As we discussed, in reinforcement learning, the agent model is informed of the immediate reward ( $R$ ) after taking an action  $a$  [27]. Rewards are essential in reinforcement learning because they encourage agents to learn and explore. Without incentives, agents would have no means of recognizing which controls are crucial and they would be unlikely to progress in accomplishing their given job or resolving a particular control issue. We define the reward as

$$R = \frac{1}{L_{\cos\_sim}} \quad (6)$$

However, in a one-step game, rather than the action iteration, the agent gives the first action as policy. Thus, the first immediate reward is the discounted reward ( $G_t = R$ ).

The agent model (*Removal*) cannot directly learn from the reward, because the reward value function is non-differentiable. Therefore, the loss function that is differentiable and related to the model parameters is essential to reinforce learning, since it can compute the policy gradient value for training. In general, the RL loss function is [47]

$$L_{RL} = - \sum_{t=0}^H \nabla_{\delta} \log \pi_{\delta}(a_t | s_t) \cdot G_t \quad (7)$$

which formulates the sum of the gradient of the logarithm of the policy ( $\nabla_{\delta} \log \pi_{\delta}(a_t | s_t)$ ) with respect to the policy parameters  $\delta$  and multiply with every step's discount reward ( $G_t$ ) from the beginning until step  $H$ . Due to the input data being a pair of instruction sequences ( $I_a$  and  $I_b$ ), the output features of the *MPNetTokenizer* with *Removal* contain two token ids ( $T_a$  and  $T_b$ ), attention masks ( $M_a$  and  $M_b$ ), and probability distributions ( $p_a$  and  $p_b$ ). Based on the input and Equation 3, the RL loss function ( $L_{RL}$ ) of a one-step

game ( $H = t = 1, G_t = R$ ) can be computed by

$$\begin{aligned} L_{RL} &= -\beta_1 \cdot \nabla_{\delta} \log \pi_{\delta}(a | s) \cdot R \\ &= -\beta_1 \cdot \log \pi_{\delta}(a_{I_a} | s_{I_a}) \cdot \log \pi_{\delta}(a_{I_b} | s_{I_b}) \cdot R \\ &= -\beta_1 \cdot \log p_a \cdot \log p_b \cdot R \end{aligned} \quad (8)$$

Moreover, in the RL loss, we add  $\beta_1$  to control the learning rate of  $L_{RL}$ . After fine-tuning, the value of  $\beta_1$  is finalized at 0.05.

### 3.5 Variational Information Bottleneck with Conditions

As we discussed in Section 2, our goal is to find an optimal way to build representations of assembly functions, which keep the maximal amount of useful information about functions and remove the nuisance information at the embedding level. We adopt the Information Bottleneck (IB) [46] theory in our work. Since we aim to implement a model that performs well for out-of-domain architectures and libraries, we require the model to learn the key features of paired instruction sequences without the nuisance information from their architectures, because this redundant information may negatively affect the performance of our model [40]. Hence, using identical encoding as the stochastic representation of the input instruction sequences is not reasonable, even though this can solve the problems caused by the invariance of the mutual information to parameterizations [4]. Instead, we use an information constraint,  $C$ , to constrain the mutual information  $M_u$  between the encoding and the input source. We embed the tokens from *Removal* to embeddings  $E$  by the MPNet encoder as input sources and try to generate an encoding  $Z$  that is maximally informative about learning target  $Y$  [4], so we have the objective function below.

$$\max M_u(Z, Y) \text{ s.t. } M_u(E, Z) \leq C \quad (9)$$

Then, based on Information Bottleneck (IB) method [46], our goal is that the encoding  $Z$  could be maximally informative representations of our learning targets  $Y$  and maximally compress the redundant information in  $E$  [4]. Therefore, a Lagrange parameter,  $\beta_2$ , is to control the trade-off: the larger the  $\beta_2$  is, the more highly compressed representations will be generated [4]. By this means, the IB objective function becomes

$$IB = M_u(Z, Y) - \beta_2 M_u(Z, E). \quad (10)$$

In the above function, the  $M_u(Z, Y)$  part simulates the  $Z$  to be the representation with the most useful information of  $Y$ , and  $\beta_2 M_u(Z, E)$  penalizes the representation for transmitting useless information from  $E$  [4]. Alemi *et al.* [4] in 2017 proposed a practical way, called Variational Information Bottleneck (VIB), which seeks to acquire an effective latent representation of the input data for the downstream learning tasks by using variational inference [40]. The VIB model proposed by Alemi *et al.* [4] has two essential components. One is a stochastic encoder, denoted by  $p(Z|E)$  that converts input data into a low-dimensional representation and identifies an optimal latent representation of the input data. The other one is a decoder, or a predictor, denoted by  $q(Y|Z)$ , that converts the low-dimensional representation back to the initial data space and is taught to recreate the input data from the representation while keeping the key features [4, 40]. The major goal of variational approaches is to convert inference into an optimization problem.

Based on the VIB method [4], the mutual information between encoding and the target  $M_u(Z, Y)$  is defined as

$$M_u(Z, Y) = \int dy dz p(y, z) \log \frac{p(y | z)}{p(y)} \quad (11)$$

where  $e, z$  and  $y$  are the instances of  $E, Z$  and  $Y$ .

There is an intractable posterior probability distribution,  $p(y|z)$  in our case. Variational approaches will attempt to find one variational approximation,  $q(z|e)$ , which is the optimal and tractable representation of the true posterior [31]. Thus, known Kullback-Leibler (KL) divergence is always greater or equal to zero, the  $KL[p(Y|Z), q(Y|Z)] \geq 0$  [4] inequality equation can be written to

$$\int dy p(y|z) \log p(y|z) \geq \int dy p(y|z) \log q(y|z) \quad (12)$$

As it is an optimization problem, based on the above equations and empirical distribution function, the loss function for VIB [4] is

$$L_{VIB} = \frac{1}{N} \sum_{n=1}^N \left[ \int dz p(z|e_n) \log q(y_n|z) - \beta_2 p(z|e_n) \log \frac{p(z|e_n)}{r(z)} \right] \quad (13)$$

where  $r(z)$  is the variational approximation to the marginal distribution of  $Z$ , and  $N$  represents the number of inputs. We use a reparameterization technique [29] that samples from a noise distribution  $\epsilon$  and then transforms it using a differentiable function dependent on the encoder network’s parameters, resulting in a sample that approximates the desired distribution. The mathematical expression of the reparameterization trick on distribution  $e$  by using the same deterministic neural network  $f(e)$  used in the encoder is [40]

$$f(e) = \mu_z(e) + \sigma_z(e) \cdot \epsilon_z \quad (14)$$

where  $\mu_z$  and  $\sigma_z$  are the mean and standard deviation of the distribution, respectively, and  $\epsilon_z$  is a sample from a noise distribution [29].

This trick allows the gradients to be backpropagated through the encoder network, enabling it to be trained using stochastic gradient descent [4]. Overall, the final objective function of VIB is [4]

$$J_{IB} = \frac{1}{N} \sum_{n=1}^N \mathbb{E}_{\epsilon \sim p(\epsilon)} [-\log q(y_n | f(e_n, \epsilon))] + \beta_2 KL[p(Z|e_n), r(Z)] \quad (15)$$

However, unsupervised learning is not well-suited for our task because while training, we lose control of VIB, so it may remove the useful information about instruction sequences and concentrate on the information about architectures and optimizations. This situation varies depending on the data, which is contrary to our original goal (removing only information related to architectures and optimizations from encoding). Therefore, in order to control the information which should be kept and which should be “forgotten”, inspired by conditional Variational Auto-Encoder (CVAE) [37], we add conditions, i.e., labels indicating the architectures or optimizations of each paired assembly code to the VIB encoder. We thus named this new method Conditional Variational Information Bottleneck (CVIB). However, unlike CVAE, condition labels are only inputted during the training phase, and not used during testing.

Similar to VIB, the encoder of the Variational Autoencoder (VAE) [29] receives source data and generates probability distributions in the latent space, while the decoder receives points in the latent space

and returns artificial data. Consequently, for a given image, the encoder generates a distribution, a point in the latent space is sampled from this distribution, and this point is then transmitted to the decoder, which generates an artificial image [18]. VAE decoder denoted by  $Q(o|v)$  aims to reconstruct  $o$  from the unobserved latent variables,  $v$ , and its encoder is thus denoted by  $P(v|o)$ . Hence, the flow in the VAE would be  $o \rightarrow v \rightarrow o'$  where  $o'$  represents the reconstructed image. Based on notions, the loss function of VAE can be defined as [37]

$$L_{VAE} = \mathbb{E}_P[\log Q(o|v)] - KL(P(v|o)|Q(v)) \quad (16)$$

However, the decoder can only produce a random digit image as its output. CVAE solves this problem by introducing the condition labels, denoted by  $l$ , in both the encoder and decoder. So the system relies on both the latent space and the extra inputs  $l$  to encode input data  $P(v|l, o)$  and decode to the target value  $Q(o|l, v)$ . In this case, CVAE can generate digit images according to the user’s demands [18, 37]. Mathematically, the variational objective of CVAE is formulated as [37]

$$L_{CVAE} = \mathbb{E}_P[\log Q(o|l, v)] - KL(P(v|l, o)|Q(v|l)) \quad (17)$$

Analogous to this method, components of the VIB model can be conditioned on a couple of observed labels (architecture label  $l_a$  and optimization label  $l_o$ ) to learn/forget target information. However, the difference between conditions in CVAE and CVIB is that conditions in CVIB are only used during the training phase, not the testing phase. In addition, we only add conditions in the *CVIBEncoder* because the CVAE’s goal is to reconstruct the input image, so it needs the conditions in the decoder to produce the full image by controlling the conditions. However, in our case, we focus on the representations  $Z$  of the instruction embeddings  $E$  in the VIB instead of the reconstructed data  $o'$  in the VAE. Thus, we do not need the condition labels inputted to the *CVIBDecoder*.

Hence, given the fact that our input is a pair of instruction embeddings encoded by *MPNetEmbedder*, then  $N = 2$ , based on Equation 17, 15 and 13 and the previous statement, we propose the CVIB (conditions in training only) information loss function as

$$L_{CVIB} = \frac{1}{2} \cdot \sum_{n=1}^2 \left[ \int dz p(z|e_n, l_a, l_o) \log q(y_n|z) - \beta_2 \cdot p(z|e_n, l_a, l_o) \log \frac{p(z|e_n, l_a, l_o)}{r(z|l_a, l_o)} \right] \quad (18)$$

and the CVIB (conditions in training only) final objective function

$$J_{CVIB} = -\frac{1}{2} \cdot \sum_{n=1}^N \mathbb{E}_{\epsilon \sim p(\epsilon)} [\log q(y_n|f(e_n, \epsilon))] + \beta_2 \cdot KL[p(Z|e_n, l_a, l_o), r(Z|l_a, l_o)] \quad (19)$$

### 3.6 Semantic Search

Semantic search is the query-answer searching technique that captures the meanings of query and entries to improve the performance of the model, as opposed to lexical search, which seeks exact matches of the query terms or similar phrases, without comprehending the context of the question [6]. Its goal is to find the most related answer to the query in a corpus of entries. For its mechanism, all of the entries in the corpus would be embedded into a

**Table 1: The Distributions of Architectures and Libraries in Training and Out-of-Domain Datasets**

| Dataset       | architectures   | libraries                      |
|---------------|-----------------|--------------------------------|
| Training      | ARM, AMD64, x86 | busybox, OpenSSL, splite3      |
| OOD-ARCH      | PowerPC, MIPS   | busybox, OpenSSL, splite3      |
| OOD-LIBS      | ARM, AMD64, x86 | putty, coreutils, curl, magick |
| OOD-ARCH&LIBS | PowerPC, MIPS   | putty, coreutils, curl, magick |

vector space. Also, the query is embedded into the same vector space during the search, and the closet embeddings from the corpus to the query embedding are identified as the output answer because they have high semantic overlapping with each other [41]. Specifically, the semantic search utilizes the cosine similarity function to compute similarity scores between the query embedding and all embeddings of entries in the corpus. It then chooses the entry that has the highest similarity score as output [41].

We adopt this method to measure the similarity score between two encodings of input assembly functions generated from *CVIBEncoder*. We treat the first instruction embedding  $Z_a$  as the query and the second  $Z_b$  as the answer entry. Afterwards, instead of collecting the top entry, we treat its similarity score in the range  $[0, 1]$  as *score*.

## 4 EXPERIMENT

### 4.1 Data Preparation and Evaluation Setups

To evaluate our models’ performance under real-world circumstances, we collect open-source projects from different vendors/libraries, which are Busybox, OpenSSL, Putty, Curl, Coreutils, sqlite3, and ImageMagick, and for different architectures (ARM, x86, MIPS, PowerPC, AMD64). We then use the IDA pro disassembler [12] to unzip and extract “asm.json.gz” files which contain the assembly function code from the packages. Then, we build a File2Ins model to merge all instructions of an assembly function into a sequence and store the path, function name, and instruction sequence in a dictionary. Afterwards, we use different filters to categorize assembly functions in the same architecture or from the same libraries into groups. Based on sorted assembly functions, we generate our pair-wise training and out-of-domain tests.

**4.1.1 File2Ins.** In the phase of assembly data extraction, we collect pieces of instructions from blocks and merge instructions into a long string in the order of blocks’ calls and addresses. Also, when collecting assembly functions, we would skip the functions that have less than ten blocks because they are too small to provide sufficiently useful information to learn.

**4.1.2 Out-of-domain Tests.** In statistics and machine learning, out-of-domain tests, often referred to as out-of-domain validation, are a method for evaluating how well a prediction model performs on data that was not utilized during its training phase [8].

In the last phase of the data preprocessing, we adopt the out-of-domain strategy and create three pair-wise out-of-domain tests and

eight sub-validations to evaluate our models. Our goal is to assure models could have higher accuracy and Area Under the receiver operating characteristic Curve (AUC) values than other baselines. Given two assembly functions' information, we set the ground truth value either by 1 (if two functions are functional/semantic similar) or by 0 (they are functional/semantic dissimilar) based on the functions' names. Also, all datasets are balanced (the ratio of label 1 and label 0 is 1: 1). The details of architectures and libraries used for training and out-of-domain testings are shown in Table 1. When building our training dataset, we select assembly functions derived from libraries (BusyBox, OpenSSL, and splite3) and ARM, AMD64, and x86 as three assembly architectures, using assembly functions derived from the same libraries and architectures of PowerPC and MIPS for the out-of-domain architecture test (OOD-ARCH), using assembly functions from different libraries (Putty, CoreUtils, Curl, and Magick) and from the same architectures for then out-of-domain libraries test (OOD-LIB), and using assembly functions from different libraries (Putty, CoreUtils, etc.) and from different architectures (MIPS and PowerPC) as out-of-domain architecture and libraries test (OOD-ARCH&LIB).

Moreover, since we generate OOD-ARCH and OOD-LIB test sets by randomly selecting eligible assembly functions and pairing them together, paired data in these sets may have the same or different architectures and optimization flags (O0, O1, O2, and O3). For instance, one pair of assembly functions in OOD-ARCH may both have x86 architectures but different optimization flags, O1 and O0. Hence, we filter the OOD-ARCH and OOD-LIB datasets and split them into four subsets by the same/different architecture and same/different optimizations, marked as OOD-ARCH-sameA, OOD-ARCH-diffA, OOD-ARCH-sameO, OOD-ARCH-diffO, OOD-LIB-sameA, OOD-LIB-diffA, OOD-LIB-sameO, OOD-LIB-diffO.

## 4.2 Benchmark Setup

Aiming to show the improvement *Pluvio* achieved, we select several state-of-the-art approaches as baseline schemes, and we split some of them into sub-baselines by utilizing different combinations of components.

**Order Matters** [51]: This method pre-trains a BERT language model on the assembly code, passes the embeddings to a GRU-based Message Passing Neural Network (MPNN) layer, combines with the order embeddings from an 11-layer ResNet model on a CFG adjacency matrix, and get final embeddings from a fully connected layer for the final output.

**OM(BERT)**: This method is a sub-model of the ORDER MATTERS model [51], which uses a basic BERT model without pre-training, passes the embeddings to a GRU-based Message Passing Neural Network (MPNN) layer, combines with the order embeddings from an 11-layer ResNet model on a CFG adjacency matrix, and get final embeddings from a fully connected layer for the final output.

**OM(ResNet7)**: This method is a sub-model of the ORDER MATTERS model [51], which pre-trains a BERT language model on the assembly code, passes the embeddings to a GRU-based Message Passing Neural Network (MPNN) layer, combines with the order embeddings from a 7-layer ResNet model on a CFG adjacency matrix, and get final embeddings from a fully connected layer for the final output.

**ResNet11**: This method is a sub-model of the ORDER MATTERS model [51], which uses only the order embeddings from an 11-layer ResNet model on a CFG adjacency matrix.

**PalmTree** [33]: This method adopts three pre-training tasks on the BERT model to capture the embeddings of assembly code to calculate the cosine similarity degree.

**SAFE** [35]: This method combines embeddings of assembly functions generated by the word2vec model and block embedding created by a self-attentive neural network to calculate the cosine similarity between assembly functions.

**Asm2Vec** [17]: This method generates embeddings of assembly code by using an unsupervised-learning PV-DM model.

**MPNet** [41]: The *all-mpnet-base-v2* sentence transformer, built based on the *mpnet-base* model and trained on a large and diverse dataset of over 1 billion training pairs, published by Hugging Face [25]. We use this model to generate embeddings of the assembly code and then compute function similarity degrees.

**MPNet-QA** [41]: The *multi-qa-mpnet-base-dot-v1* sentence transformer model, built based on the *mpnet-base* model and tuned for specific tasks, semantic search, by pre-training on a large and diverse set of question and answer pairs. We use this model to generate embeddings of assembly code and calculate function similarity.

**DistilRoBERTa** [41]: The *all-distilroberta-v1* is one of the distilled versions of the RoBERTa-base models and trained on a large and diverse dataset of over 1 billion training pairs, totalling 82M parameters [42]. We use this model to generate embeddings of assembly code and calculate function similarity.

**Distil-ML** [41]: The *distiluse-base-multilingual-cased-v2* is a Multi-Lingual model of Universal Sentence Encoder for 15 different languages (Chinese, Dutch, English, etc), which is published by Hugging Face [25]. We use this model to generate embeddings of assembly code and calculate function similarity.

**MiniLM** [41]: The *all-MiniLM-L12-v2* sentence transformer trains on very large sentence-level datasets using a self-supervised contrastive learning objective, published by Hugging Face [25]. We use this model to generate embeddings of assembly code and calculate function similarity.

## 4.3 Evaluation Metrics

We choose to adopt the confusion matrix to evaluate the performance of our models, since it can precisely analyze the potential of a classifier by comparing the ground truth (0 and 1 in our task) and predicted labels (similarity degree score in the range of 0 and 1) of assembly code embeddings. The efficiency of the classifier is determined with regard to the following metrics generated from the confusion matrix entries [5]. Accuracy is the percentage of correctly classified pairs; Precision is the proportion of correctly classified positive cases among all predicted positive cases; Recall is the proportion of correctly classified positive cases among all actual positive cases; then F1-score is a balanced measure (harmonic mean) of precision and recall. Overall, the higher the values, the better performance the model achieves.

Besides the four entries above, we also employ the area under a receiver operating characteristic (ROC) curve, abbreviated as AUC, as an important evaluator to measure the overall performance of our models [36]. Because its computation is based on the whole

**Table 2: Performance of Baseline Models and *Pluvio* on Out-of-Domain Architecture Tests with the Same and Different Architectures (OOD-ARCH-sameA and OOD-ARCH-diffA)**

| Model              | out-of-domain architectures<br>(same architecture within a pair) |              |              |              |              | out-of-domain architectures<br>(different architecture within a pair) |              |              |              |              |
|--------------------|--|--------------|--------------|--------------|--------------|---|--------------|--------------|--------------|--------------|
|                    | auc  | accu         | prc          | rcl          | f1           | auc   | accu         | prc          | rcl          | f1           |
| OM(RESNET7) [51]   | 0.685  | 0.634        | 0.601        | 0.609        | 0.543        | 0.505   | 0.527        | 0.524        | 0.517        | 0.451        |
| OM(BERT) [51]      | 0.651  | 0.581        | 0.560        | 0.554        | 0.481        | 0.479   | 0.487        | 0.503        | 0.483        | 0.429        |
| ORDER MATTERS [51] | 0.706  | 0.643        | 0.627        | 0.631        | 0.622        | 0.537   | 0.510        | 0.553        | 0.532        | 0.541        |
| RESNET11 [51]      | 0.531  | 0.504        | 0.499        | 0.480        | 0.416        | 0.390   | 0.401        | 0.436        | 0.432        | 0.379        |
| PALMTREE [33]      | 0.688  | 0.681        | 0.844        | 0.386        | 0.529        | 0.544   | 0.543        | 0.585        | 0.556        | 0.570        |
| SAFE [35]          | 0.500  | 0.500        | 0.000        | 0.000        | 0.000        | 0.500   | 0.500        | 0.000        | 0.000        | 0.000        |
| ASM2VEC [17]       | 0.497  | 0.553        | 0.000        | 0.000        | 0.000        | 0.505   | 0.501        | 0.545        | 0.505        | 0.524        |
| MPNet [41]         | 0.914  | 0.845        | 0.861        | 0.774        | 0.817        | 0.838   | 0.765        | 0.796        | 0.764        | 0.780        |
| MPNet-QA [41]      | 0.853  | 0.836        | 0.805        | 0.822        | 0.803        | 0.787   | 0.717        | 0.735        | 0.625        | 0.730        |
| DistilRoBERTa [41] | 0.919  | 0.848        | 0.840        | 0.815        | 0.827        | 0.821   | 0.739        | 0.789        | 0.711        | 0.748        |
| Distil-ML [41]     | 0.851  | 0.078        | 0.755        | 0.756        | 0.756        | 0.728   | 0.669        | 0.703        | 0.678        | 0.690        |
| MiniLM [41]        | 0.804  | 0.741        | 0.733        | 0.662        | 0.698        | 0.673   | 0.633        | 0.667        | 0.649        | 0.658        |
| <b>Pluvio</b>      | <b>0.942</b>   | <b>0.866</b> | <b>0.844</b> | <b>0.860</b> | <b>0.852</b> | <b>0.876</b>  | <b>0.795</b> | <b>0.803</b> | <b>0.827</b> | <b>0.815</b> |

**Table 3: Performance of Baseline Models and *Pluvio* on Out-of-Domain Architecture Tests with the Same and Different Optimizations (OOD-ARCH-sameO and OOD-ARCH-diffO)**

| Model              | out-of-domain architectures<br>(same optimization within a pair) |              |              |              |              | out-of-domain architectures<br>(different optimization within a pair) |              |              |              |              |
|--------------------|--|--------------|--------------|--------------|--------------|---|--------------|--------------|--------------|--------------|
|                    | auc  | accu         | prc          | rcl          | f1           | auc   | accu         | prc          | rcl          | f1           |
| OM(RESNET7) [51]   | 0.693  | 0.643        | 0.627        | 0.634        | 0.562        | 0.684   | 0.636        | 0.603        | 0.612        | 0.542        |
| OM(BERT) [51]      | 0.664  | 0.603        | 0.578        | 0.569        | 0.502        | 0.653   | 0.583        | 0.5630       | 0.557        | 0.485        |
| ORDER MATTERS [51] | 0.715  | 0.667        | 0.648        | 0.645        | 0.637        | 0.710   | 0.649        | 0.526        | 0.636        | 0.634        |
| RESNET11 [51]      | 0.54   | 0.516        | 0.510        | 0.500        | 0.422        | 0.537   | 0.509        | 0.504        | 0.486        | 0.418        |
| PALMTREE [33]      | 0.748  | 0.686        | 0.924        | 0.514        | 0.569        | 0.701   | 0.653        | 0.892        | 0.384        | 0.537        |
| SAFE [35]          | 0.500  | 0.500        | 0.000        | 0.000        | 0.000        | 0.500   | 0.000        | 0.000        | 0.000        | 0.000        |
| ASM2VEC [17]       | 0.752  | 0.505        | 0.003        | 0.000        | 0.005        | 0.496   | 0.477        | 0.000        | 0.000        | 0.000        |
| MPNet [41]         | 0.944  | 0.942        | 0.932        | 0.937        | 0.921        | 0.940   | 0.865        | 0.898        | 0.838        | 0.867        |
| MPNet-QA [41]      | 0.963  | 0.944        | 0.956        | 0.982        | 0.905        | 0.937   | 0.862        | 0.892        | 0.836        | 0.863        |
| DistilRoBERTa [41] | 0.962  | 0.920        | 0.922        | 0.945        | 0.904        | 0.942   | 0.874        | 0.909        | 0.844        | 0.875        |
| Distil-ML [41]     | 0.931  | 0.866        | 0.844        | 0.895        | 0.883        | 0.853   | 0.782        | 0.826        | 0.739        | 0.780        |
| MiniLM [41]        | 0.837  | 0.737        | 0.825        | 0.765        | 0.711        | 0.812   | 0.735        | 0.795        | 0.667        | 0.725        |
| <b>Pluvio</b>      | <b>0.972</b>   | <b>0.949</b> | <b>0.953</b> | <b>0.944</b> | <b>0.936</b> | <b>0.945</b>  | <b>0.870</b> | <b>0.888</b> | <b>0.861</b> | <b>0.878</b> |

ROC curve and therefore takes into account all potential classification thresholds, the AUC is a reliable overall metric to assess the effectiveness of score classifiers. Typically, the AUC is determined by multiplying successive trapezoid regions beneath the ROC curve [36]. In contrast to accuracy, AUC ranks the predictions rather than just calculating their absolute values to quantify the quality of the model’s predictions independent of the categorization threshold applied. Due to the classification-threshold-invariance and scale-invariance of AUC, it is a desirable evaluator to our task [14, 20].

#### 4.4 Overall Performance

In the experiment, we evaluate all baselines model and *Pluvio* performances on eight different out-of-domain tests, and all testing sets contain the balanced and pair-wise assembly instruction sequences from different architectures, libraries and optimizations. In Table 2, the two columns of results, including Area Under ROC, accuracy, precision, recall and F-1 score, show the performance of the models

on out-of-domain architectures (OOD-ARCH), and their names are placed correspondingly on the left part. As we claimed, the filter is applied on the OOD-ARCH test to divide the test into two sub-tests, i.e., the same architecture pairs and the different architecture pairs. The middle column in Table 2 displays models’ performances on the OOD-ARCH with the same architecture pairs (OOD-ARCH-sameA) and the OOD-ARCH-diffA on the right column. Overall, all models perform worse in different architecture pairs than in the same pairs, due to the inconsistency of architecture types. Even so, *Pluvio* still achieves the best performances (94.2% and 87.6% in AUC, 86.6% and 79.5% in accuracy) among all the models. The same happens in the remaining three OOD tests shown in Table 3, Table 4, and Table 5.

*Pluvio* achieves outstanding performance in every out-of-domain test, which demonstrates its effectiveness and robustness. By looking at our baseline and the state-of-the-art models, the series of the sentence transformers [41] show good performance, especially

**Table 4: Performance of Baseline Models and *Pluvio* on Out-of-Domain Libraries Tests with the Same and Different Architectures (OOD-LIBS-sameA and OOD-LIBS-diffA)**

| Model              | out-of-domain libraries<br>(same architecture within a pair) |              |              |              |              | out-of-domain libraries<br>(different architecture within a pair) |              |              |              |              |
|--------------------|--|--------------|--------------|--------------|--------------|---|--------------|--------------|--------------|--------------|
|                    | auc  | accu         | prc          | rcl          | f1           | auc   | accu         | prc          | rcl          | f1           |
| OM(RESNET7) [51]   | 0.693  | 0.647        | 0.617        | 0.624        | 0.549        | 0.654   | 0.632        | 0.615        | 0.560        | 0.540        |
| OM(BERT) [51]      | 0.661  | 0.593        | 0.578        | 0.563        | 0.502        | 0.662   | 0.591        | 0.5764       | 0.563        | 0.501        |
| ORDER MATTERS [51] | 0.715  | 0.664        | 0.639        | 0.644        | 0.638        | 0.711   | 0.667        | 0.636        | 0.599        | 0.620        |
| RESNET11 [51]      | 0.546  | 0.513        | 0.517        | 0.499        | 0.427        | 0.541   | 0.506        | 0.513        | 0.467        | 0.421        |
| PALMTREE [33]      | 0.510  | 0.324        | 0.456        | 0.412        | 0.366        | 0.417   | 0.319        | 0.312        | 0.480        | 0.353        |
| SAFE [35]          | 0.500  | 0.500        | 0.000        | 0.000        | 0.000        | 0.500   | 0.500        | 0.000        | 0.000        | 0.000        |
| ASM2VEC [17]       | 0.506  | 0.506        | 0.738        | 0.506        | 0.601        | 0.4111  | 0.497        | 0.000        | 0.000        | 0.000        |
| MPNet [41]         | 0.935  | 0.872        | 0.943        | 0.879        | 0.900        | 0.915   | 0.856        | 0.925        | 0.862        | 0.8295       |
| MPNet-QA [41]      | 0.922  | 0.845        | 0.941        | 0.841        | 0.888        | 0.888   | 0.874        | 0.878        | 0.832        | 0.714        |
| DistilRoBERTa [41] | 0.816  | 0.824        | 0.848        | 0.804        | 0.858        | 0.802   | 0.819        | 0.863        | 0.782        | 0.755        |
| Distil-ML [41]     | 0.904  | 0.820        | 0.930        | 0.816        | 0.869        | 0.891   | 0.952        | 0.838        | 0.804        | 0.724        |
| MiniLM [41]        | 0.899  | 0.081        | 0.925        | 0.817        | 0.867        | 0.857   | 0.784        | 0.740        | 0.807        | 0.692        |
| <b>Pluvio</b>      | <b>0.955</b>   | <b>0.894</b> | <b>0.958</b> | <b>0.933</b> | <b>0.913</b> | <b>0.934</b>  | <b>0.873</b> | <b>0.942</b> | <b>0.914</b> | <b>0.881</b> |

**Table 5: Performance of Baseline Models and *Pluvio* on Out-of-Domain Libraries Tests with the Same and Different Optimizations (OOD-LIBS-sameO and OOD-LIBS-diffO)**

| Model              | out-of-domain libraries<br>(same optimization within a pair) |              |              |              |              | out-of-domain libraries<br>(different optimization within a pair) |              |              |              |              |
|--------------------|--|--------------|--------------|--------------|--------------|---|--------------|--------------|--------------|--------------|
|                    | auc  | accu         | prc          | rcl          | f1           | auc   | accu         | prc          | rcl          | f1           |
| OM(RESNET7) [51]   | 0.688  | 0.640        | 0.613        | 0.622        | 0.551        | 0.664   | 0.612        | 0.573        | 0.600        | 0.518        |
| OM(BERT) [51]      | 0.653  | 0.596        | 0.561        | 0.555        | 0.482        | 0.638   | 0.5662       | 0.554        | 0.527        | 0.462        |
| ORDER MATTERS [51] | 0.706  | 0.656        | 0.635        | 0.633        | 0.625        | 0.694   | 0.621        | 0.508        | 0.614        | 0.612        |
| RESNET11 [51]      | 0.537  | 0.501        | 0.509        | 0.492        | 0.413        | 0.511   | 0.487        | 0.489        | 0.460        | 0.403        |
| PALMTREE [33]      | 0.805  | 0.785        | 0.785        | 0.666        | 0.880        | 0.578   | 0.423        | 0.929        | 0.201        | 0.329        |
| SAFE [35]          | 0.500  | 0.500        | 0.000        | 0.000        | 0.000        | 0.500   | 0.500        | 0.000        | 0.000        | 0.000        |
| ASM2VEC [17]       | 0.503  | 0.512        | 0.787        | 0.518        | 0.625        | 0.499   | 0.293        | 0.000        | 0.000        | 0.000        |
| MPNet [41]         | 0.955  | 0.912        | 0.962        | 0.924        | 0.942        | 0.922   | 0.847        | 0.935        | 0.842        | 0.886        |
| MPNet-QA [41]      | 0.952  | 0.936        | 0.956        | 0.962        | 0.959        | 0.903   | 0.812        | 0.921        | 0.802        | 0.858        |
| DistilRoBERTa [41] | 0.953  | 0.891        | 0.963        | 0.895        | 0.928        | 0.895   | 0.805        | 0.926        | 0.788        | 0.851        |
| Distil-ML [41]     | 0.912  | 0.821        | 0.951        | 0.813        | 0.877        | 0.898   | 0.812        | 0.921        | 0.803        | 0.858        |
| MiniLM [41]        | 0.913  | 0.870        | 0.914        | 0.890        | 0.915        | 0.886   | 0.811        | 0.898        | 0.827        | 0.841        |
| <b>Pluvio</b>      | <b>0.960</b>   | <b>0.920</b> | <b>0.964</b> | <b>0.933</b> | <b>0.948</b> | <b>0.926</b>  | <b>0.858</b> | <b>0.924</b> | <b>0.869</b> | <b>0.896</b> |

the *all-mpnet-base-v2* model. This is because they consist of hundreds of MPNet layers and are pre-trained by huge and various training pairs, over 1 billion diverse training datasets that equip the sentence transformers [41] with high generalizability. However, they are designed as general-purpose models, not specifically for assembly code clone search. In contrast, *Pluvio* is pre-trained by only a trivial number of training data pairs compared to 1 billion and acquires greater generalizability (79.5%, 87.0%, 87.3% and 85.8% in accuracy in all four “out-of-same different architectures and optimizations” tests compared to 76.5%, 86.5%, 85.6% and 84.7%) than the pre-trained sentence transformers. Then, for the ORDER MATTERS [51] model and its three sub-models, OM(RESNET7) [51], OM(BERT) [51] and RESNET11 [51], achieve only at most 71.5% in AUC among all eight sub-tests. In the training phase, ORDER MATTERS [51] extracts and combines the semantic-aware, structure-aware and order-aware embeddings from CFGs of assembly functions to measure the similarity degree, which improves the richness

of embeddings information. This strategy disregards the intricate intra-instruction structures and relies heavily on the control flow, where contextual information is noisy and subject to influence from compiler optimizations [33]. Thus, plenty of noisy information from architectures, libraries, and optimizations would mix into the embeddings, disturbing the model to lose focus. Out-of-domain tests clearly present this shortcoming in ORDER MATTERS [51]. Then, for the PALMTREE MODEL [33], it realizes this problem, but only works on solving the impact of compiler optimizations and leaves the architectures for their future work. Hence, from Table 5, we could see that the PALMTREE MODEL [33] reaches 80.5% AUC in the OOD-LIBS-sameO test, outperforming ORDER MATTERS [51] (70.6% in AUC). However, in the out-of-domain tests with regard to architectures, the PALMTREE [33] model can only achieve 51.0% and 41.7% for the AUC in OOD-LIBS-sameA and OOD-LIBS-diffA tests. Focusing on obfuscations and not considering the impacts of different architectures, libraries, and optimizations, ASM2VEC [17]

**Table 6: Performance of Baseline Models *Pluvio* on Out-of-Domain Architectures and Libraries Test (OOD-ARCH&LIB)**

| Model              | out-of-domain architecture and libraries |              |              |              |              |
|--------------------|--|--------------|--------------|--------------|--------------|
|                    | auc                                      | accu         | prc          | rcl          | f1           |
| OM(RESNET7) [51]   | 0.497                                    | 0.528        | 0.523        | 0.390        | 0.437        |
| OM(BERT) [51]      | 0.485                                    | 0.516        | 0.522        | 0.358        | 0.426        |
| ORDER MATTERS [51] | 0.507                                    | 0.549        | 0.524        | 0.469        | 0.453        |
| RESNET11 [51]      | 0.425                                    | 0.507        | 0.523        | 0.324        | 0.327        |
| PALMTREE [33]      | 0.488                                    | 0.543        | 0.517        | 0.142        | 0.237        |
| SAFE [35]          | 0.500                                    | 0.500        | 0.000        | 0.000        | 0.000        |
| ASM2VEC [17]       | 0.499                                    | 0.500        | 0.000        | 0.000        | 0.000        |
| MPNet [41]         | 0.831                                    | 0.765        | 0.746        | 0.801        | 0.772        |
| MPNet-QA [41]      | 0.834                                    | 0.766        | 0.776        | 0.749        | 0.762        |
| DistilRoBERTa [41] | 0.822                                    | 0.755        | 0.771        | 0.727        | 0.748        |
| Distil-ML [41]     | 0.607                                    | 0.575        | 0.550        | 0.823        | 0.659        |
| MiniLM [41]        | 0.5794                                   | 0.567        | 0.544        | 0.828        | 0.656        |
| <b>Pluvio</b>      | <b>0.887</b>                             | <b>0.825</b> | <b>0.833</b> | <b>0.813</b> | <b>0.823</b> |

**Table 7: Ablation Test for *Pluvio* on Out-of-Domain Architectures and Libraries. All models are trained by the balanced pair-wise assembly functions training dataset and tested by the OOD-ARCH&LIBS set.**

| Model  | out-of-domain architectures and libraries |              |              |              |              |
|--|---|--------------|--------------|--------------|--------------|
|  | auc                                       | accu         | prc          | rcl          | f1           |
| <i>Pluvio-Removal-CVIB</i><br>-Semantic search | 0.736                                     | 0.700        | 0.696        | 0.735        | 0.715        |
| <i>Pluvio-Removal-CVIB</i>                     | 0.766                                     | 0.739        | 0.731        | 0.771        | 0.749        |
| <i>Pluvio-CVIB</i>                             | 0.843                                     | 0.813        | 0.807        | 0.810        | 0.809        |
| <b>Pluvio</b>                                  | <b>0.887</b>                              | <b>0.825</b> | <b>0.833</b> | <b>0.813</b> | <b>0.823</b> |

performs poorly in all OOD tests as well. For example, in the OOD-LIBS-diffA test in Table 4, the Recall, Precision and F1-score of ASM2VEC [17] are approaching zeros because nearly none of “similar” (label=1) class is classified correctly. SAFE [35] has the same or even worse situation. It gives “0s” for every testing pair in all datasets. Since all testing sets are balanced (having 50% similar (1) and 50% dissimilar (0) testing pairs), SAFE [35] achieves only 50.0% in AUC and accuracy and 0.0% in the remaining three metrics in all OOD tests. Due to being pre-trained by over one million assembly code lines [35], SAFE is overfitting to a specific compiler architecture and loses its generalizability in all other architectures, as well as for optimizations and libraries.

Table 6 gives a comprehensive view of all models’ performance since it evaluates the models on both out-of-domain architectures and libraries. From this table, *Pluvio* achieves 88.7% in AUC and 82.5% in accuracy, resulting in more than 35 percent improvement compared to the existing state-of-the-art models. Because of *Removal* and CVIB (conditions in training only), nuisance information is removed at both the token and embedding levels, and the key features maximally informative about assembly functions are kept. In this way, *Pluvio* consistently achieves outstanding performance in all tests, proving its reliability and practicability in real-world assembly code clone search and all downstream works.

## 4.5 Ablation Test

To evaluate the necessity and performance of each component in *Pluvio*, we exert the ablation test on the out-of-domain architectures and libraries (OOD-ARCH&LIBS) and display the results in Table 7. In Table 7, the “-” means without. For instance, *Pluvio-CVIB* means the *Pluvio* model without the CVIB (conditions in training only) part. Since Table 6 and Table 7 are on the same testing set, we could observe that *Pluvio-Removal-CVIB-semantic search*, even without the *Removal*, CVIB (conditions in training only) and semantic search, outperforms (73.6% in AUC and 70.0% in accuracy) the state-of-the-art models. After adding the semantic search back, the model does not achieve obvious improvements in overall performance, because semantic search is the extended work of cosine similarity. Then, adding the *Removal* back, the agent model removes noise tokens and at this time, *Pluvio-CVIB* already surpasses all baseline models, including sentence transformers [41], showing the importance of *Removal* module. At last, the complete *Pluvio* achieves further giant progress in all aspects with the help of CVIB (conditions in training only).

## 5 CONCLUSION

In this paper, we propose a robust and effective assembly code clone search engine, namely *Pluvio*. We combine the pre-trained natural language model, transfer learning, reinforcement learning, and a novel method, which is a conditional variational information bottleneck, to create the embeddings from any given assembly function. *Pluvio* introduces a new perspective to generate robust instruction embeddings by removing the nuisance information in the assembly functions. *Removal* extracts a set of the top important tokens of the assembly function, so the impact of inlining functions and compiler-injected code can be mitigated. By conditional variational information bottleneck, *Pluvio* is conditioned on learning the true semantics of assembly functions in the latent space and creates embeddings without nuisance information of architectures, libraries, and optimizations. *Pluvio* accepts not only the assembly functions, but also basic blocks, function segments, or even multiple lines of code as input without any extra information. We perform out-of-domain testing on assembly code clone search, utilizing a variety of compiler architectures, libraries, and optimizations. The convincing results demonstrate that *Pluvio* is a robust and effective assembly code clone search engine which accurately classifies assembly codes in unseen architectures or from unseen libraries.

## REFERENCES

- [1] 2017. Cosine distance cosine similarity angular cosine distance angular cosine similarity.
- [2] Saurabh Agarwala, Aniketh Anagawadi, and Ram Mohana Reddy Guddeti. 2021. Detecting Semantic Similarity Of Documents Using Natural Language Processing. *Procedia Computer Science* 189 (2021), 128–135.
- [3] Suneet Agrawal. 2020. Inline function: Kotlin.
- [4] Alexander A. Alemi, Ian Fischer, Joshua V. Dillon, and Kevin Murphy. 2017. Deep Variational Information Bottleneck. In *5th International Conference on Learning Representations* (Toulon, France).
- [5] Siddhartha Kumar Arjaria, Abhishek Singh Rathore, and Jincy S. Cherian. 2021. Chapter 13 - Kidney disease prediction using a machine learning approach: A comparative and comprehensive analysis. In *Demystifying Big Data, Machine Learning, and Deep Learning for Healthcare Analytics*. Academic Press, 307–333.
- [6] Hannah Bast, Björn Buchhold, and Elmar Haussmann. 2016. Semantic Search on Text and Knowledge Bases. *Found. Trends Inf. Retr.* 10, 2-3 (2016), 119–271.
- [7] Peter J. Bickel. 2015. Mathematical statistics. (2015).
- [8] Jason Brownlee. 2021. How to use out-of-fold predictions in machine learning.

- [9] David Brumley, Pongsin Pooankam, Dawn Xiaodong Song, and Jiang Zheng. 2008. Automatic Patch-Based Exploit Generation is Possible: Techniques and Implications. In *2008 IEEE Symposium on Security and Privacy* (Oakland, CA). IEEE, 143–157.
- [10] Danilo Bruschi, Lorenzo Martignoni, and Mattia Monga. 2006. Detecting Self-mutating Malware Using Control-Flow Graph Matching. In *Detection of Intrusions and Malware & Vulnerability Assessment, Third International Conference, DIMVA 2006, Berlin, Germany, July 13-14, 2006, Proceedings (Lecture Notes in Computer Science, Vol. 4064)*. Springer, 129–143.
- [11] William Y. Chen, Pohua P. Chang, Thomas M. Conte, and Wen-mei W. Hwu. 1993. The Effect of Code Expanding Optimizations on Instruction Cache Design. *IEEE Trans. Computers* 42, 9 (1993), 1045–1057.
- [12] Eagle Chris. 2008. The IDA pro book The unofficial guide to the world’s most popular disassembler.
- [13] Nullstone Corporation. 2012. Function inlining.
- [14] Google Developer. 2020. Classification: ROC curve and AUC. *Google* (Feb 2020).
- [15] Jacob Devlin, Ming-Wei Chang, Kenton Lee, and Kristina Toutanova. 2018. BERT: Pre-training of Deep Bidirectional Transformers for Language Understanding. *CoRR abs/1810.04805* (2018).
- [16] Steven H. H. Ding, Benjamin C. M. Fung, and Philippe Charland. 2016. Kam1n0: MapReduce-based Assembly Clone Search for Reverse Engineering. In *Proceedings of the 22nd ACM SIGKDD International Conference on Knowledge Discovery and Data Mining, San Francisco, CA, USA, August 13-17, 2016*. ACM, 461–470.
- [17] Steven H. H. Ding, Benjamin C. M. Fung, and Philippe Charland. 2019. Asm2Vec: Boosting Static Representation Robustness for Binary Clone Search against Code Obfuscation and Compiler Optimization. In *2019 IEEE Symposium on Security and Privacy, SP 2019, San Francisco, CA, USA, May 19-23, 2019*. IEEE, 472–489.
- [18] Isaac Dykeman. 2016. Conditional variational autoencoders.
- [19] Omar Espejel and Nils Reimers. 2022. Sentence-transformers/all-mpnet-base-V2.
- [20] Tom Fawcett. 2006. An introduction to ROC analysis. *Pattern Recognit. Lett.* 27, 8 (2006), 861–874.
- [21] Garron Fish. 2020. A closer look at Inline.
- [22] Jiawei Han, Micheline Kamber, and Jian Pei. 2012. Chapter 2: Getting to Know Your Data. In *Data Mining* (third edition ed.). Morgan Kaufmann, Boston, 39–82.
- [23] Irfan Ul Haq and Juan Caballero. 2019. A Survey of Binary Code Similarity. *CoRR abs/1909.11424* (2019).
- [24] Yikun Hu, Yuanyuan Zhang, Juanru Li, and Dawu Gu. 2016. Cross-Architecture Binary Semantics Understanding via Similar Code Comparison. In *IEEE 23rd International Conference on Software Analysis, Evolution, and Reengineering, SANER 2016, Suita, Osaka, Japan, March 14-18, 2016 - Volume 1*. IEEE Computer Society, 57–67.
- [25] HuggingFace. 2016. Hugging face hub documentation.
- [26] IBM. 2018. What does it mean to inline a function and how does it affect a program.
- [27] Leslie Pack Kaelbling, Michael L. Littman, and Andrew W. Moore. 1996. Reinforcement Learning: A Survey. *J. Artif. Intell. Res.* 4 (1996), 237–285.
- [28] Rashi Karanpuria. 2021. Learning Kotlin: Inline functions.
- [29] Diederik P. Kingma and Max Welling. 2014. Auto-Encoding Variational Bayes. In *2nd International Conference on Learning Representations, ICLR 2014, Banff, AB, Canada, April 14-16, 2014, Conference Track Proceedings*.
- [30] Charles W. Krueger. 1992. Software reuse. *Comput. Surveys* 24, 2 (1992), 131–183.
- [31] Volodymyr Kuleshov. 2023. Variational inference.
- [32] Quoc V. Le and Tomas Mikolov. 2014. Distributed Representations of Sentences and Documents. In *Proceedings of the 31th International Conference on Machine Learning, ICML 2014, Beijing, China, 21-26 June 2014 (JMLR Workshop and Conference Proceedings, Vol. 32)*. JMLR.org, 1188–1196.
- [33] Xuezixiang Li, Yu Qu, and Heng Yin. 2021. PalmTree: Learning an Assembly Language Model for Instruction Embedding. In *CCS ’21: 2021 ACM SIGSAC Conference on Computer and Communications Security, Virtual Event, Republic of Korea, November 15 - 19, 2021*. ACM, 3236–3251.
- [34] Lannan Luo, Jiang Ming, Dinghao Wu, Peng Liu, and Sencun Zhu. 2017. Semantics-Based Obfuscation-Resilient Binary Code Similarity Comparison with Applications to Software and Algorithm Plagiarism Detection. *IEEE Trans. Software Eng.* 43, 12 (2017), 1157–1177.
- [35] Luca Massarelli, Giuseppe Antonio Di Luna, Fabio Petroni, Roberto Baldoni, and Leonardo Querzoni. 2019. SAFE: Self-Attentive Function Embeddings for Binary Similarity. In *Detection of Intrusions and Malware, and Vulnerability Assessment - 16th International Conference, DIMVA 2019, Gothenburg, Sweden, June 19-20, 2019, Proceedings (Lecture Notes in Computer Science, Vol. 11543)*. Springer, 309–329.
- [36] Francisco Melo. 2013. *Area under the ROC Curve*. Springer New York, 38–39.
- [37] Artidoro Pagnoni, Kevin Liu, and Shangyan Li. 2018. Conditional Variational Autoencoder for Neural Machine Translation. *CoRR abs/1812.04405* (2018).
- [38] Kexin Pei, Zhou Xuan, Junfeng Yang, Suman Jana, and Baishakhi Ray. 2020. Trex: Learning Execution Semantics from Micro-Traces for Binary Similarity. *CoRR abs/2012.08680* (2020).
- [39] Jannik Pewny, Behrad Garmany, Robert Gawlik, Christian Rossow, and Thorsten Holz. 2015. Cross-Architecture Bug Search in Binary Executables. In *2015 IEEE Symposium on Security and Privacy*. 709–724.
- [40] Weizhu Qian and Franck Gechter. 2020. Variational Information Bottleneck Model for Accurate Indoor Position Recognition. In *25th International Conference on Pattern Recognition, ICPR 2020, Virtual Event / Milan, Italy, January 10-15, 2021*. IEEE, 2529–2535.
- [41] Nils Reimers and Iryna Gurevych. 2019. Sentence-BERT: Sentence Embeddings using Siamese BERT-Networks. In *Proceedings of the 2019 Conference on Empirical Methods in Natural Language Processing*. Association for Computational Linguistics.
- [42] Victor Sanh, Lysandre Debut, Julien Chaumond, and Thomas Wolf. 2019. DistilBERT, a distilled version of BERT: smaller, faster, cheaper and lighter. *ArXiv abs/1910.01108* (2019).
- [43] Manuel Sojer and Joachim Henkel. 2010. Code reuse in open source software development: Quantitative evidence, drivers, and impediments. *Journal of the Association for Information Systems* 11, 12 (2010), 868–901.
- [44] Kaitao Song, Xu Tan, Tao Qin, Jianfeng Lu, and Tie-Yan Liu. 2020. MPNet: Masked and Permuted Pre-training for Language Understanding. *CoRR abs/2004.09297* (2020).
- [45] Richard S. Sutton and Andrew G. Barto. 1998. *Reinforcement learning - an introduction*. MIT Press.
- [46] Naftali Tishby, Fernando C. N. Pereira, and William Bialek. 2000. The information bottleneck method. *CoRR physics/0004057* (2000).
- [47] Jordi TORRES.AI. 2021. Policy-gradient methods.
- [48] Ashish Vaswani, Noam Shazeer, Niki Parmar, Jakob Uszkoreit, Llion Jones, Aidan N. Gomez, Lukasz Kaiser, and Illia Polosukhin. 2017. Attention is All you Need. In *Advances in Neural Information Processing Systems 30: Annual Conference on Neural Information Processing Systems 2017, December 4-9, 2017, Long Beach, CA, USA*. 5998–6008.
- [49] Xiaojun Xu, Chang Liu, Qian Feng, Heng Yin, Le Song, and Dawn Song. 2017. Neural Network-based Graph Embedding for Cross-Platform Binary Code Similarity Detection. In *Proceedings of the 2017 ACM SIGSAC Conference on Computer and Communications Security, CCS 2017, Dallas, TX, USA, October 30 - November 03, 2017*. ACM, 363–376.
- [50] Zhilin Yang, Zihang Dai, Yiming Yang, Jaime G. Carbonell, Ruslan Salakhutdinov, and Quoc V. Le. 2019. XLNet: Generalized Autoregressive Pretraining for Language Understanding. In *Advances in Neural Information Processing Systems 32: Annual Conference on Neural Information Processing Systems 2019, NeurIPS 2019, December 8-14, 2019, Vancouver, BC, Canada*. 5754–5764.
- [51] Zeping Yu, Rui Cao, Qiyi Tang, Sen Nie, Junzhou Huang, and Shi Wu. 2020. Order Matters: Semantic-Aware Neural Networks for Binary Code Similarity Detection. In *The Thirty-Fourth AAAI Conference on Artificial Intelligence, AAAI 2020, The Thirty-Second Innovative Applications of Artificial Intelligence Conference, IAAI 2020, The Tenth AAAI Symposium on Educational Advances in Artificial Intelligence, EAAI 2020, New York, NY, USA, February 7-12, 2020*. 1145–1152.
- [52] Fei Zuo, Xiaopeng Li, Patrick Young, Lannan Luo, Qiang Zeng, and Zhixin Zhang. 2019. Neural machine translation inspired binary code similarity comparison beyond function pairs. *Network and Distributed System Security Symposium* (2019).